

SCIENTIFIC REPORTS



OPEN

Fast non-Abelian geometric gates via transitionless quantum driving

J. Zhang^{1,2}, Thi Ha Kyaw², D. M. Tong¹, Erik Sjöqvist^{3,4} & Leong-Chuan Kwek^{2,5,6,7}

Received: 30 June 2015

Accepted: 17 November 2015

Published: 21 December 2015

A practical quantum computer must be capable of performing high fidelity quantum gates on a set of quantum bits (qubits). In the presence of noise, the realization of such gates poses daunting challenges. Geometric phases, which possess intrinsic noise-tolerant features, hold the promise for performing robust quantum computation. In particular, quantum holonomies, i.e., non-Abelian geometric phases, naturally lead to universal quantum computation due to their non-commutativity. Although quantum gates based on adiabatic holonomies have already been proposed, the slow evolution eventually compromises qubit coherence and computational power. Here, we propose a general approach to speed up an implementation of adiabatic holonomic gates by using transitionless driving techniques and show how such a universal set of fast geometric quantum gates in a superconducting circuit architecture can be obtained in an all-geometric approach. Compared with standard non-adiabatic holonomic quantum computation, the holonomies obtained in our approach tends asymptotically to those of the adiabatic approach in the long run-time limit and thus might open up a new horizon for realizing a practical quantum computer.

Fast and robust quantum gates play a central role in realizing a practical quantum computer. While the robustness offers resilience to certain errors such as parameter fluctuations, the fast implementation of designated quantum gates increases computational speed, which in turn decreases environment-induced errors. A possible approach towards robust quantum computation is to implement quantum gates by means of different types of geometric phases^{1–4}; an approach known as holonomic quantum computation (HQC)^{5–10}. Such geometric gates depend solely on the path of a system evolution, rather than its dynamical details.

Universal quantum computation based purely on geometric means has been proposed in the adiabatic regime, resulting in a precise control of a quantum-mechanical system⁷. Despite the appealing features, the adiabatic evolution is associated with long run time, which increases the exposure to detrimental decoherence and noise. However, this drawback can be eliminated by using non-adiabatic HQC schemes based on Abelian^{8,9} or non-Abelian geometric phases¹⁰. The latter has been developed further in refs 11–14 experimentally demonstrated in refs 15–18 and its robustness to a variety of errors has been studied in refs 19,20.

Adiabatic processes can also be carried out swiftly by employing transitionless quantum driving algorithm (TQDA) if the quantum system consists of non-degenerate subspaces²¹. This is also known as adiabatic shortcut in the literature^{22–27}. A key notion of TQDA is to seek a transitionless Hamiltonian so that the system evolves exactly along the same adiabatic passage of a given target Hamiltonian, but at any desired rate. This is achieved with the aid of an additional Hamiltonian that suppresses the energy level fluctuations caused by the changes in the system parameters.

In this report, we generalize TQDA to degenerate subspaces, where non-Abelian geometric phases are acquired after a cyclic evolution. With the help of the generalized TQDA, we propose a universal set of non-adiabatic holonomic single- and two-qubit gates. Specifically, non-Abelian geometric phases or quantum holonomies are acquired by a degenerate subspace after a cyclic evolution. TQDA-based geometric phases are realized via non-adiabatic evolution, dictated by an additional transition-suppressing Hamiltonian. We further simplify the transitionless Hamiltonian by selectively choosing geodesic path segments forming a loop in the system parameter space. This

¹Department of Physics, Shandong University, Jinan 250100, China. ²Centre for Quantum Technologies, National University of Singapore, 3 Science Drive 2, Singapore 117543, Singapore. ³Department of Quantum Chemistry, Uppsala University, Box 518, Se-751 20 Uppsala, Sweden. ⁴Department of Physics and Astronomy, Uppsala University, Box 516, Se-751 20 Uppsala, Sweden. ⁵MajuLab, CNRS-UNS-NUS-NTU International Joint Research Unit, UMI 3654, Singapore. ⁶Institute of Advanced Studies, Nanyang Technological University, 60 Nanyang View, Singapore 639673, Singapore. ⁷National Institute of Education, Nanyang Technological University, 1 Nanyang Walk, Singapore 637616, Singapore. Correspondence and requests for materials should be addressed to D.M.T. (email: tdm@sdu.edu.cn) or E.S. (email: erik.sjoqvist@physics.uu.se) or L.-C.K. (email: cqtklc@nus.edu.sg)

effectively reduces the complexity of the control parameters, which in turn simplifies the physical implementation of the TQDA-gates. Finally, we show how to realize the effective Hamiltonians in superconducting tunable coupling transmons.

Results

Degenerate TQDA. Let us consider a quantum-mechanical system characterized by a Hamiltonian $H_0(\vec{\lambda})$ that depends on a set of control parameters $\vec{\lambda}$. For an eigenvalue $E_n(\vec{\lambda})$ of the Hamiltonian, we assume there exists a set of m_n eigenstates $|\varphi_k^n(\vec{\lambda})\rangle$ ($k = 1, \dots, m_n$) that span the proper subspace \mathcal{M}_n of Hilbert space \mathcal{H} . When the parameter $\vec{\lambda}$ is varied from an initial value $\vec{\lambda}_i$ to a final value $\vec{\lambda}_f$, the adiabatic theorem entails that \mathcal{M}_n does not mix with other subspaces in \mathcal{H} when the corresponding run time tends to infinity. The states $|\varphi_k^n\rangle$ satisfying the Schrödinger equation along the path in parameter space are related to $|\varphi_k^n\rangle$ as $|\varphi_k^n\rangle = \sum_l |\varphi_l^n\rangle C_{lk}^n$ with C^n being unitary matrices. By substituting this relation into the Schrödinger equation, we arrive at

$$C^n = \mathcal{T} \exp\left(-\int A^n dt\right), \quad (1)$$

up to a global dynamical phase. Here, \mathcal{T} is a time-ordering operator, the connection $A_{kl}^n = \langle \varphi_k^n | \dot{\varphi}_l^n \rangle$ is an anti-Hermitian $m_n \times m_n$ matrix, and we have assumed the initial condition $C^n(0) = \hat{1}^n$, $\hat{1}^n$ being the $m_n \times m_n$ unit matrix. We focus on a cyclic adiabatic evolution, i.e., $\vec{\lambda}_f = \vec{\lambda}_i$. A non-trivial transformation relating the initial and final states is a quantum gate. This transformation operator, be it Abelian ($m_n = 1$) or non-Abelian ($m_n \geq 2$), is a quantum holonomy.

The transitionless Hamiltonian that exactly generates the adiabatic time evolution governed by the unitary operator $U = \sum_{n,k} |\varphi_k^n\rangle \langle \varphi_k^n(0)|$, can be obtained by reverse engineering²¹ yielding

$$H = H_0 + H_1 = \sum_{n,k} E_n |\varphi_k^n\rangle \langle \varphi_k^n| + i \sum_{n,k,l} (|\dot{\varphi}_k^n\rangle \langle \varphi_k^n| - A_{kl}^n |\varphi_k^n\rangle \langle \varphi_l^n|). \quad (2)$$

Since we have made no assumptions regarding the dimensionality m_n of the subspaces, this result generalizes Berry's TQDA²¹ to the degenerate case. From this point onwards, we denote $H_0 = \sum_{n,k} E_n |\varphi_k^n\rangle \langle \varphi_k^n|$ as the target Hamiltonian. One notes that the expectation values $\langle \varphi_k^n | H | \varphi_k^n \rangle$ and $\langle \varphi_k^n | H_0 | \varphi_k^n \rangle$ coincide, i.e., the dynamical phases acquired are the same, although the eigenstates $|\varphi_k^n\rangle$ of H_0 are not eigenstates of the transitionless Hamiltonian H . In cyclic evolution, a non-Abelian geometric phase, induced by the matrix-valued connection appearing in the additional transition-suppressing Hamiltonian, is picked up by each subspace. In the following, we demonstrate how to arrive at desired quantum gates from non-Abelian geometric phases under the degenerate TQDA.

Fast holonomic single-qubit gates. To implement our proposed holonomic gates, we consider a generic system consisting of four bare energy eigenstates $|0\rangle$, $|1\rangle$, $|a\rangle$, and $|e\rangle$, coupled by external oscillating fields in a tripod configuration⁷. Here, $|0\rangle$, $|1\rangle$ are qubit states; $|e\rangle$ and $|a\rangle$ are excited and auxiliary states, respectively. By assuming that all fields are resonant with the transitions, the target Hamiltonian of such a system is written as

$$H_0 = \Omega |e\rangle \langle e| + f_{e0} |0\rangle \langle 0| + f_{e1} |1\rangle \langle 1| + f_{ea} |a\rangle \langle a| + \text{H.c.}, \quad (3)$$

where each f_{kl} serves as a time-dependent control parameter for the $l \leftrightarrow k$ transition in a frame that rotates with the fields. H_0 has two dark and two bright eigenstates, and the former eigenstates provide a proper subspace to encode a qubit. To obtain our desired holonomic gates, we evolve the subspace along some loops in parameter space. In the standard adiabatic scheme⁷, this task is accomplished by changing the control parameters slowly so that transitions between the dark and bright subspaces become negligible. In the following, we show explicitly how to speed up this process with the help of degenerate TQDA. Since the qubit information is stored in the dark subspace, there is no dynamical contribution. Therefore, the desired quantum holonomy is acquired at the end of the evolution in the same manner as in ref. 7.

We first construct a phase-shift gate $U_P = e^{i\gamma_1 |1\rangle \langle 1|}$, where the phase γ_1 depends solely on the path in the parameter space defined by the f_{kl} 's. This holonomic gate is implemented adiabatically with the Λ -like Hamiltonian $H_0^P = \Omega_1 |e\rangle \langle e| \left(-\sin \frac{\theta}{2} e^{i\varphi} |1\rangle \langle 1| + \cos \frac{\theta}{2} |a\rangle \langle a|\right) + \text{H.c.}$, where the state $|0\rangle$ is decoupled ($f_{e0} = 0$). The Hamiltonian H_0^P has a parameter-dependent dark eigenstate $|D\rangle = \cos \frac{\theta}{2} |1\rangle + \sin \frac{\theta}{2} e^{i\varphi} |a\rangle$, and two bright eigenstates. The dark state $|D\rangle$ initially coincides with $|1\rangle$ by choosing $\theta = \varphi = 0$ at $t = 0$. After completing a cyclic adiabatic evolution, this qubit state acquires the Berry phase factor $e^{i\gamma_1} = e^{-\frac{i}{2} \int_S \sin \theta d\theta d\varphi}$, with S being the surface enclosed by the path shown in Fig. 1(a). Thus, γ_1 is minus half the solid angle enclosed on the parameter sphere with polar angles θ and φ .

The shortcut to this adiabatic process is realized by adding an extra Hamiltonian term H_1^P to the target Hamiltonian H_0^P . It is evident that H_1^P relies both on the structure and rate of change of H_0^P . In order to simplify H_1^P , we propose evolving the system in three steps forming an "orange slice" path on the parameter sphere along which the connection A vanishes (see Fig. 1(a,b) and Supplementary information for details). First, $\varphi = 0$ while changing θ from 0 to π . During this step, terms containing $\dot{\varphi}$ and $\sin \varphi$ vanish, and $H^P = H_0^P + H_1^P$ becomes a Δ -like Hamiltonian, in which the Rabi frequency between $|1\rangle$ and $|a\rangle$ is $\dot{\theta}/2$. Therefore, a $1 \leftrightarrow a$ transition is added to the system caused by the temporal change in θ . In the second step, we keep $\theta = \pi$, but vary φ from 0 to φ_1 . Here, the total Hamiltonian is just a transition between $|e\rangle$ and $|1\rangle$ with detuning $\dot{\varphi}$. Thus, the detuning is caused by the

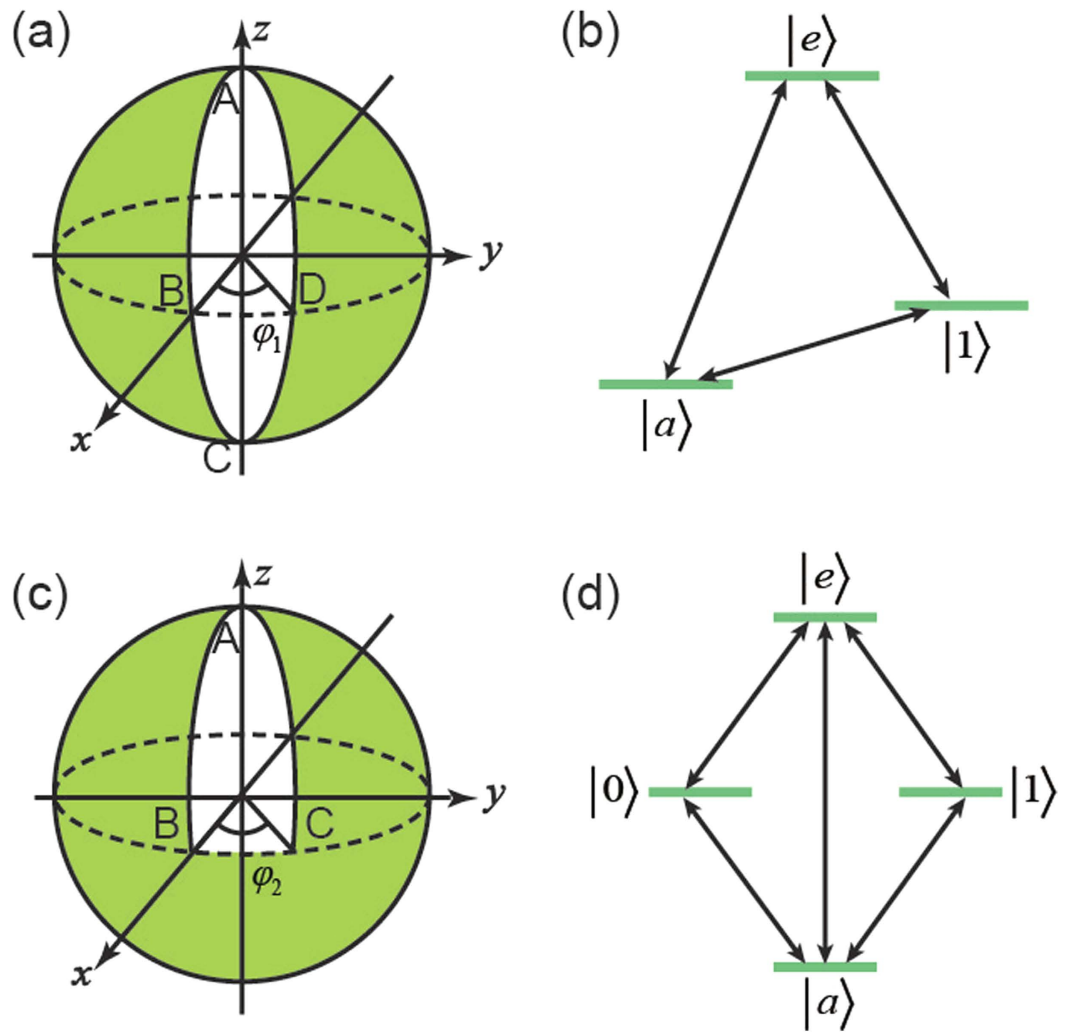


Figure 1. Schematic diagram for the orange slice and geodesic triangle schemes. The spheres in (a,c) represent the parameter space, where the control parameters θ and φ are changed following a specific path. When we set $\theta = \varphi = 0$, the starting point in the parameter space is along the z axis. The parameters θ and φ are polar angle and azimuthal angle in the parameter space, respectively. (a) Schematic diagram for the orange slice scheme. The state $|1\rangle$ is evolved by changing the parameters along the path A-B-C-D-A. The opening angle is φ_1 . (b) The level structure for the first and third steps in achieving U_p . Transitions between all three levels are needed, which makes it a Δ model Hamiltonian. (c) Schematic diagram for the geodesic triangle scheme. The manifold, consisting of $|0\rangle$ and $|1\rangle$, is evolved by changing the parameters along the path A-B-C-A, while the opening angle is φ_2 . (d) The level structure for the last step in achieving U_B . Transitions between all four levels are needed.

temporal change in the parameter φ . Finally, we keep $\varphi = \varphi_1$, while θ is decreased to 0. During this final step, H^P is again a Δ -like Hamiltonian. When $\theta = 0$, H^P has returned to its initial form. As shown in Fig. 1(a), the acquired geometric phase γ_1 is equal to minus the azimuthal angle φ_1 , i.e., minus half the solid angle enclosed by the orange slice shaped loop. We note that both the detuning in the second step and the $1 \leftrightarrow a$ transition in the first and third steps are caused by the fast parameter change. Thus, H_0^P is recovered in the adiabatic limit when the rate of the parameter change tends to zero. The steps of the control Hamiltonian needed to implement U_p are shown in Table 1.

Similarly, an adiabatic gate $U_B = e^{i\gamma_2\sigma_y}$, $\sigma_y = i(|0\rangle\langle 1| - |1\rangle\langle 0|)$ can be realized by utilizing the full tripod structure with $f_{e0} = \Omega \sin \theta \cos \varphi$, $f_{e1} = \Omega \sin \theta \sin \varphi$, and $f_{ea} = \Omega \cos \theta$. This Hamiltonian has two degenerate parameter-dependent dark eigenstates, which we take as $|D_1\rangle = \cos \theta (\cos \varphi |0\rangle + \sin \varphi |1\rangle) - \sin \theta |a\rangle$ and $|D_2\rangle = \cos \varphi |1\rangle - \sin \varphi |0\rangle$, together with two non-degenerate bright eigenstates. Similar to the adiabatic phase-shift gate, our qubit is encoded within the dark subspace. The desired holonomic gate is obtained after traversing a loop on the parameter sphere with polar angles θ and φ , resulting in γ_2 as the solid angle swept⁷.

Shortcut to U_B is realized by choosing a geodesic triangle path on the corresponding parameter sphere, again in order to force the connection A to vanish (see Fig 1(c,d) and Supplementary information for details). The purpose of this choice is to simplify the implementation of the gate, just as the choice of an “orange slice” path simplified

	Step1	Step2	Step3
U_P	$ e\rangle \leftrightarrow 1\rangle, e\rangle \leftrightarrow a\rangle, 1\rangle \leftrightarrow a\rangle$	$ e\rangle \leftrightarrow 1\rangle$	$ e\rangle \leftrightarrow 1\rangle, e\rangle \leftrightarrow a\rangle, 1\rangle \leftrightarrow a\rangle$
U_B	$ e\rangle \leftrightarrow 0\rangle, e\rangle \leftrightarrow a\rangle, 0\rangle \leftrightarrow a\rangle$	$ e\rangle \leftrightarrow 0\rangle, e\rangle \leftrightarrow 1\rangle, 0\rangle \leftrightarrow 1\rangle$	$ e\rangle \leftrightarrow 0\rangle, e\rangle \leftrightarrow 1\rangle, e\rangle \leftrightarrow a\rangle, 0\rangle \leftrightarrow a\rangle, 1\rangle \leftrightarrow a\rangle$

Table 1. Transitions needed in the “orange slice” scheme and the “geodesic triangle” scheme. The “orange slice” scheme and the “geodesic triangle” scheme are proposed to achieve the single qubit gates U_P and U_B , respectively. Each scheme contains three steps and needed transitions for each step are listed. The symbol $|i\rangle \leftrightarrow |j\rangle$ denotes the transition between the states $|i\rangle$ and $|j\rangle$.

the implementation of U_P . Initially, we set $\theta = \varphi = 0$, which implies $|D_1\rangle = |0\rangle$ and $|D_2\rangle = |1\rangle$, followed by increasing θ to $\frac{\pi}{2}$, while keeping φ constant. During this step, $H^B = H_0^B + H_1^B$ exhibits a Δ -like structure involving the states $|e\rangle$, $|0\rangle$, and $|a\rangle$. Thereafter, we keep θ unchanged but rotate φ to φ_2 . H^B has again a Δ -like structure, but now involving $|e\rangle$, $|0\rangle$, and $|1\rangle$. Finally, θ is decreased to zero along the geodesic curve and then φ is tuned to zero. The level structure for the last step is depicted in Fig. 1(d). Unlike the “orange slice” scheme, no detuning emerges in the “geodesic triangle” scheme. Therefore, all the photon-assisted transitions are resonant. The steps of the control Hamiltonian needed to implement U_B are shown in Table. 1. We may note that all transitions between the four levels $|0\rangle$, $|1\rangle$, $|a\rangle$, and $|e\rangle$ are needed to realize an arbitrary single-qubit gate by combining U_P and U_B .

Fast holonomic two-qubit gate. Since the combination of the gates U_P and U_B allows the realization of an arbitrary single-qubit gate, it remains to construct an entangling two-qubit holonomic gate to realize universal quantum computation^{28,29}. A holonomic two-qubit gate can be realized in the TQDA scenario, by controlling suitable coupling parameters between two four-level tripod systems. Specifically, we note that there are four auxiliary states, $\mathcal{K} = \{|e\rangle_l \otimes |e\rangle_r, |e\rangle_l \otimes |a\rangle_r, |a\rangle_l \otimes |e\rangle_r, |a\rangle_l \otimes |a\rangle_r\}$ from the two four-level systems (see Methods and Supplementary information for details). The key idea is to construct a Δ -like structure to combine two auxiliary states from \mathcal{K} and one of the two-qubit states. The target Hamiltonian of the two-qubit gate can be taken as $H_0^2 = J_1|ea\rangle\langle 10| + J_2|ea\rangle\langle ae| + H.c.$ By using the same “orange slice” scheme as in the realization of U_P , a geometric phase is acquired by the state $|10\rangle$ while the other states remain unchanged. This amounts to applying an entangling gate $U_2 = e^{i\gamma_3|10\rangle\langle 10|}$ on the two-qubit space, where γ_3 is the geometric phase obtained after the cyclic evolution.

The single- and two-qubit gates in superconducting circuits. To realize our non-adiabatic schemes experimentally, we consider a superconducting tunable coupling transmon (TCT)³⁰ (see Fig. 2(a)), in which we assume that the transition frequency of the system and system-resonator coupling strength can be tuned independently. In the symmetric configuration, where $E_{J_a}^1 = E_{J_a}^2 = E_{J_a}^0$, $a = \pm$, the system Hamiltonian is described by^{30,31}

$$H_0^{\text{TCT}} = \sum_{a=\pm} \left[4E_{C_a}(n_a - n_{g_a})^2 - E_{J_a}^0 \cos(\pi f_a) \cos(\gamma_a - 2\pi f_a) \right] + 4E_I n_+ n_-, \quad (4)$$

where E_{C_a} are the charging energies of the upper and lower islands, while $E_{J_a}^i$, $i = 1, 2$, are the Josephson energies (see Methods for definition of the other parameters in H_0^{TCT}). In the limit of large $E_{J_a}^a/E_{C_a}$, the energy level splitting is observed with increase in E_I as shown in Fig. 3(a), giving rise to the four energy levels $|0\rangle$, $|1\rangle$, $|a\rangle$ and $|e\rangle$ needed to implement our proposal.

When a time-dependent microwave field $\Phi(t)$ impinges onto our four-level TCT (see Figs 2(a) and 3(a) and Methods), microwave-assisted transitions occur. To investigate allowed energy level transitions, we consider a situation where there is a minimum flux entering the upper SQUID loop ($\Phi_+ \approx 0$), where a small change of flux (Φ_-) is present in the lower one. In this case, the perturbation Hamiltonian with small $\Phi(t)$ becomes $H_1^{\text{TCT}}(\gamma_-, t) = \Phi^{(0)} \Gamma \cos(\omega_{kl}t)$ with $\Phi^{(0)}$ the microwave amplitude, ω_{kl} a carrier frequency of the incoming microwave pulse that connects two desired eigenstates $|k\rangle$ and $|l\rangle$, and $\Gamma = (E_{J_-}/\Phi_0) \cos(\pi f_-) \sin(\gamma_- - 2\pi f_-)$. In Fig. 3(b), we plot the transition matrix elements for the eigenstates of interest $|t_{kl}\rangle = |\langle k|H_1^{\text{TCT}}|l\rangle|$ versus E_{J_-}/E_C while $E_I/E_C = 0.5$ and $E_{J_{\pm}}/E_C = 100$. From this result, we conclude that a particular energy value of E_{J_-} should be tuned via the external magnetic flux, threading the lower SQUID loop, in order to give rise to the desired energy level transitions. If we confine ourselves to the selected four eigenstates, the Hamiltonian of the superconducting circuit in a rotating frame can be expressed as $H^{\text{TCT}} = H_0^{\text{TCT}} + H_1^{\text{TCT}} = \sum_{k=l=0,1,e,a} [\Omega_{kl}|k\rangle\langle l| + \text{H.c.}]$, where $\Omega_{kl} = \hbar \langle k|\Phi^{(0)}\Gamma|l\rangle/2$ is a complex Rabi frequency. When we invoke the “orange slice” and “geodesic triangle” schemes, H^{TCT} gives rise to H^P and H^B , respectively. We note that since our schemes relax the adiabatic constraint, the holonomic gates can be obtained at any speed. However, from a practical perspective, the desired gate time depends on details of the specific experimental setup such as the energy gaps and how fast we can vary the input microwave pulses.

To implement our two-qubit gate, we consider a superconducting architecture with two TCTs placed inside a coplanar resonator (see Fig. 2(b,c)). The direct coupling between the two transmons (labeled as l and r) is mediated by a cavity in the resonant regime³². With the built-in tunability of the transmons, we realize the Hamiltonian H^2 as follow. We assume that the transmon levels are anharmonic and each level transition can be tuned at will by

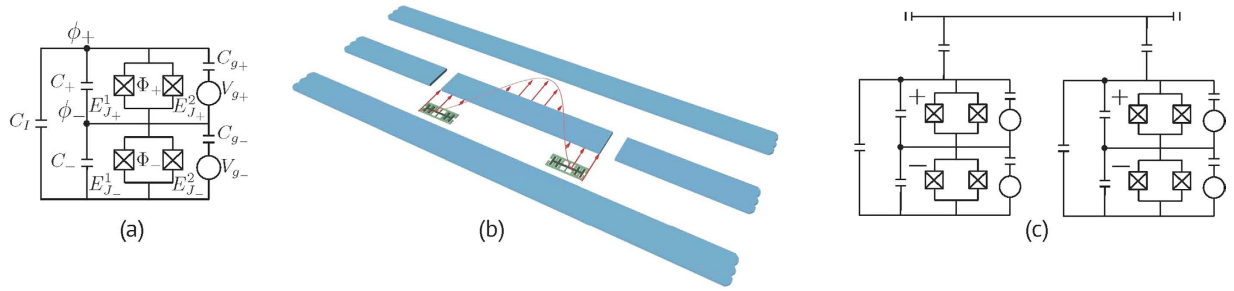


Figure 2. Diagram for superconducting circuits. (a) Circuit model of a tunable coupling transmon (TCT) system, which is used to realize our single-qubit gates in absence of a transmission line resonator. (b) A proposed setup to realize the two-qubit gate with two TCTs mediated via a resonator and (c) its equivalent circuit model, where the two TCTs are capacitively coupled to a coplanar resonator.

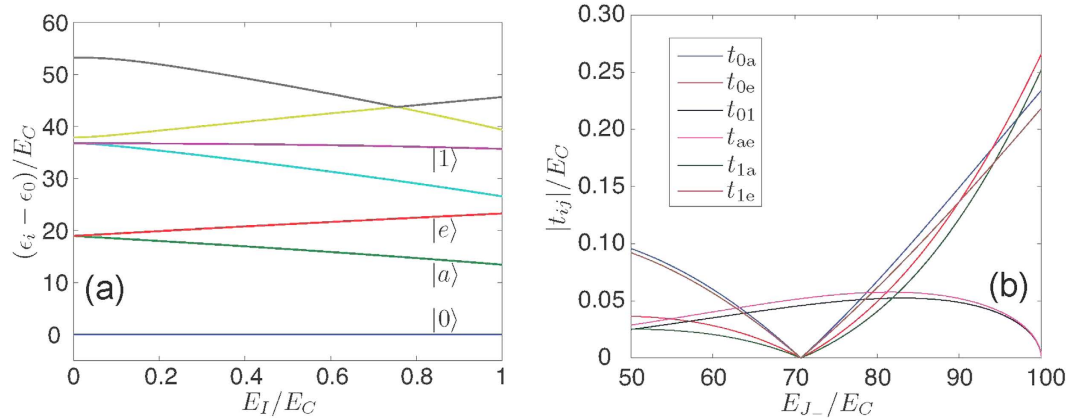


Figure 3. Energy spectrum and transition matrix for the superconducting circuits. (a) Energy spectrum of the TCT as a function of E_I/E_C for $E_{J\pm} = 50E_C$. We confine ourselves to the eigenstates $|0\rangle$, $|1\rangle$, $|e\rangle$ and $|a\rangle$. (b) Moduli $|t_{ij}|$ of the unnormalized transition matrix elements between states $|i\rangle$ and $|j\rangle$ as a function of E_{J+}/E_C for the labelled eigenstates in (b), while $E_I/E_C = 0.5$ and $E_{J-}/E_C = 100$.

matching with the resonator frequency via ac-Stark-shift fields³³, alternatively by invoking the built-in tunability of the transmons energy levels³⁰ or by tuning the resonator frequency³⁴. For instance, to achieve the transition between $|e_l, a_r\rangle$ and $|1_l, 0_r\rangle$, we switch on vacuum Rabi couplings $\hbar g_{1_l, e_l} (\sigma_{1_l, e_l}^+ a + \sigma_{1_l, e_l}^- a^\dagger)$ to transmon l , and $\hbar g_{a_r, 0_r} (\sigma_{a_r, 0_r}^+ a + \sigma_{a_r, 0_r}^- a^\dagger)$ to transmon r , where the g 's are the coupling strengths between the respective transition and the single mode resonator, $\sigma_{j,k}^+ = |j\rangle\langle k|$, $\sigma_{j,k}^- = |k\rangle\langle j|$ and a^\dagger (a) is the creation (annihilation) operator of the bosonic resonator mode, respectively. All the other required transitions can also be realized in the same manner (see Supplementary information for details).

Discussion and Conclusions

We would like to put forward some remarks on the holonomic gates based on TQDA proposed here and the nonadiabatic holonomic gates proposed in ref. 10. On one hand, we notice that both schemes are genuinely non-adiabatic in that they can be performed at any desired rate. On the other hand, the holonomies obtained in the proposed TQDA approach tends asymptotically to those of the adiabatic approach in the long run-time limit^{2,7}; a feature which is not shared by the scheme in ref. 10. As a consequence, the TQDA-based gates have an immediate geometric meaning in terms of solid angles enclosed in parameter space of the underlying target Hamiltonian, while no such explicit geometric meaning is present in the other scheme. This also makes our scheme explicitly robust to parameter fluctuations that preserve the solid angle. In addition, our scheme has the advantage over standard adiabatic scheme in that non-adiabatic transitions, which inevitably degrades the control in any realistic finite-time implementation of the adiabatic gates¹⁹, are suppressed using TQDA.

In conclusion, we have proposed a non-Abelian generalization of the TQDA and show how it can be used for holonomic quantum computation. The key feature of this algorithm is to realize quantum holonomies that can be performed at arbitrary rate by applying an additional transition-suppressing Hamiltonian so that the path of the original eigensubspaces as well as the purely geometric nature of the resulting matrix-valued phases are preserved. Non-adiabatic TQDA-based single- and two-qubit gates are proposed in a four-level transmon and two four-level transmons coupled with a cavity, respectively. With high controllability^{35,36} and scalability^{37,38} of the superconducting circuit, our scheme can also be incorporated within a more general landscape where the transmons are

embedded in a resonator lattice^{39–43}. This scheme therefore opens up new experimental horizons towards a robust all-geometric high-speed large-scale quantum computation architecture.

Methods

Superconducting tunable coupling transmon. The four level system can be provided by a superconducting tunable coupling transmon (TCT)³⁰ (see Fig. 2(a)). To obtain the effective Hamiltonian H_0^{TCT} , we define $\gamma_+ = 2\pi(\phi_+ - \phi_-)/\Phi_0$, $\gamma_- = 2\pi\phi_-/\Phi_0$ ($\Phi_0 = h/2e$ being the superconducting magnetic flux quantum) as the phase differences on the upper and lower superconducting quantum interference device (SQUID) loops, and $n_{g_{\pm}} = (C_{g_{\pm}} V_{g_{\pm}})/2e$ as the dimensionless gate voltages. The tunable Josephson energies $E_{J_{\pm}} = E_{J_{\pm}}^0 \cos(\pi f_{\pm})$, where $E_{J_{\pm}}^0 = \bar{E}_{J_{\pm}}^1 + E_{J_{\pm}}^2$ and the frustration parameters $f_{\pm} = \Phi_{\pm}/\Phi_0$, Φ_{\pm} are external magnetic fluxes threading the upper and lower superconducting quantum interference devices (SQUIDs). In H_0^{TCT} , n_{\pm} is the respective associated charge. $E_{C_{\pm}} = e^2/2C'_{\pm}$ are the charging energies of the upper and lower islands, while $E_I = -e^2/C'$ represents the interaction energy between them. By letting $C_{\Sigma_{\pm}} = C_I + C_{\pm} + C_{g_{\pm}}$, the effective capacitors C'_{\pm} and C' are defined by $C'_{\pm} = [C_{\Sigma_+} C_{\Sigma_-} - C_I^2]/C_{\Sigma_{\mp}}$ and $C' = [C_{\Sigma_+} C_{\Sigma_-} - C_I^2]/C_P$, respectively.

References

- Berry, M. V. Quantal phase factors accompanying adiabatic changes. *Proc. R. Soc. A* **392**, 45 (1984).
- Wilczek, F. & Zee, A. Appearance of gauge structure in simple dynamical systems. *Phys. Rev. Lett.* **52**, 2111 (1984).
- Aharonov, Y. & Anandan, J. Phase change during a cyclic quantum evolution. *Phys. Rev. Lett.* **58**, 1593 (1987).
- Anandan, J. Non-adiabatic non-abelian geometric phase. *Phys. Lett. A* **133**, 171 (1988).
- Zanardi, P. & Rasetti, M. Holonomic quantum computation. *Phys. Lett. A* **264**, 94 (1999).
- Jones, J. A., Vedral, V., Ekert, A. & Castagnoli, G. Geometric quantum computation using nuclear magnetic resonance. *Nature (London)* **403**, 869 (2000).
- Duan, L.-M., Cirac, J. I. & Zoller, P. Geometric manipulation of trapped ions for quantum computation. *Science* **292**, 1695 (2001).
- Wang, X. B. & Matsumoto, K. Nonadiabatic conditional geometric phase shift with NMR. *Phys. Rev. Lett.* **87**, 097901 (2001).
- Zhu, S.-L. & Wang, Z. D. Unconventional geometric quantum computation. *Phys. Rev. Lett.* **91**, 187902 (2003).
- Sjöqvist, E. *et al.* Non-adiabatic holonomic quantum computation. *New J. Phys.* **14**, 103035 (2012).
- Xu, G. F., Zhang, J., Tong, D. M., Sjöqvist, E. & Kwek, L. C. Nonadiabatic holonomic quantum computation in decoherence-free subspaces. *Phys. Rev. Lett.* **109**, 170501 (2012).
- Zhang, J., Kwek, L. C., Sjöqvist, E., Tong, D. M. & Zanardi, P. Quantum computation in noiseless subsystems with fast non-Abelian holonomies. *Phys. Rev. A* **89**, 042302 (2014).
- Xu, G. F. & Long, G. L. Protecting geometric gates by dynamical decoupling. *Phys. Rev. A* **90**, 022323 (2014).
- Xu, G. F. & Long, G. L. Universal Nonadiabatic Geometric Gates in Two-Qubit Decoherence-Free Subspaces. *Sci. Rep.* **4**, 6814 (2014).
- Abdumalikov, A. A. *et al.* Experimental realization of non-Abelian non-adiabatic geometric gates. *Nature (London)* **496**, 482 (2013).
- Feng, G., Xu, G. & Long, G. Experimental realization of nonadiabatic holonomic quantum computation. *Phys. Rev. Lett.* **110**, 190501 (2013).
- Arroyo-Camejo, S., Lazariev, A., Hell, S. W. & Balasubramanian, G. Room temperature high-fidelity holonomic single-qubit gate on a solid-state spin. *Nature Comm.* **5**, 4870 (2014).
- Zu, C. *et al.* Experimental realization of universal geometric quantum gates with solid-state spins. *Nature (London)* **514**, 72 (2014).
- Johansson, M. *et al.* Robustness of nonadiabatic holonomic gates. *Phys. Rev. A* **86**, 062322 (2012).
- Spiegelberg, J. & Sjöqvist, E. Validity of the rotating-wave approximation in nonadiabatic holonomic quantum computation. *Phys. Rev. A* **88**, 064301 (2013).
- Berry, M. V. Transitionless quantum driving. *J. Phys. A: Math. Theor.* **42**, 365303 (2009).
- Chen, X., Lizuain, I., Ruschhaupt, A., Guéry-Odelin, D. & Muga, J. G. Shortcut to adiabatic passage in two- and three-level atoms. *Phys. Rev. Lett.* **105**, 123003 (2010).
- Bason, M. G. *et al.* High-fidelity quantum driving. *Nature Phys.* **8**, 147 (2012).
- Ibáñez, S., Chen, X., Torrontegui, E., Muga, J. G. & Ruschhaupt, A. Multiple Schrödinger pictures and dynamics in shortcuts to adiabaticity. *Phys. Rev. Lett.* **109**, 100403 (2012).
- del Campo, A. Shortcuts to adiabaticity by counterdiabatic driving. *Phys. Rev. Lett.* **111**, 100502 (2013).
- Moliner, M. & Schmitteckert, P. Adiabatic Tracking of a State: A New Route to Nonequilibrium Physics. *Phys. Rev. Lett.* **111**, 120602 (2013).
- Zhang, J. *et al.* Experimental implementation of assisted quantum adiabatic passage in a single spin. *Phys. Rev. Lett.* **110**, 240501 (2013).
- Lloyd, S. Almost Any Quantum Logic Gate Is Universal. *Phys. Rev. Lett.* **75**, 346 (1995).
- Bremner, M. J. *et al.* Practical Scheme for Quantum Computation with Any Two-Qubit Entangling Gate. *Phys. Rev. Lett.* **89**, 247920 (2002).
- Gambetta, J. M., Houck, A. A. & Blais, A. Superconducting Qubit with Purcell Protection and Tunable Coupling. *Phys. Rev. Lett.* **106**, 030502 (2011).
- Devoret, M. H. *Les Houches, Session LXIII, 1995* edited by Reynaud, S., Giacobino, E. & Zinn-Justin, J. (Elsevier Science, Amsterdam, 1997), p. 351.
- Haack, G., Helmer, F., Mariantoni, M., Marquardt, F. & Solano, E. Resonant quantum gates in circuit quantum electrodynamics. *Phys. Rev. B* **82**, 024514 (2010).
- Schuster, D. I. *et al.* ac Stark Shift and Dephasing of a Superconducting Qubit Strongly Coupled to a Cavity Field. *Phys. Rev. Lett.* **94**, 123602 (2005).
- Sandberg, M. *et al.* Tuning the field in a microwave resonator faster than the photon lifetime. *Appl. Phys. Lett.* **92**, 203501 (2008).
- Barends, R. *et al.* Superconducting quantum circuits at the surface code threshold for fault tolerance. *Nature* **508**, 500 (2014).
- Chen, Y. *et al.* Qubit Architecture with High Coherence and Fast Tunable Coupling. *Phys. Rev. Lett.* **113**, 220502 (2014).
- Chow, J. M. *et al.* Implementing a strand of a scalable fault-tolerant quantum computing fabric. *Nature Comm.* **5**, 4015 (2014).
- Jeffrey, E. *et al.* Fast Accurate State Measurement with Superconducting Qubits. *Phys. Rev. Lett.* **112**, 190504 (2014).
- Helmer, F. *et al.* Cavity grid for scalable quantum computation with superconducting circuits. *Europhys. Lett.* **85**, 50007 (2009).
- Kyaw, T. H., Felicetti, S., Romero, G., Solano, E. & Kwek, L. C. Scalable quantum memory in the ultrastrong coupling regime. *Sci. Rep.* **5**, 8621 (2015).
- Paik, H. *et al.* Observation of High Coherence in Josephson Junction Qubits Measured in a Three-Dimensional Circuit QED Architecture. *Phys. Rev. Lett.* **107**, 240501 (2011).
- Koch, J. *et al.* Charge-insensitive qubit design derived from the Cooper pair box. *Phys. Rev. A* **76**, 042319 (2007).
- Stern, M. *et al.* Flux Qubits with Long Coherence Times for Hybrid Quantum Circuits. *Phys. Rev. Lett.* **113**, 123601 (2014).

Acknowledgements

J.Z. and D.M.T. acknowledge support from NSF China through Grant No. 11175105 and the National Basic Research Program of China through Grant No. 2015CB921004. T.H.K. and L.-C.K. acknowledge support from the National Research Foundation & Ministry of Education, Singapore. E.S. acknowledges financial support from the Swedish Research Council. The authors thank Guillermo Romero, Enrique Solano, Yuimaru Kubo, Patrice Bertet and Daniel Esteve for valuable discussions and helpful comments.

Author Contributions

The authors contributed equally to this work.

Additional Information

Supplementary information accompanies this paper at <http://www.nature.com/srep>

Competing financial interests: The authors declare no competing financial interests.

How to cite this article: Zhang, J. *et al.* Fast non-Abelian geometric gates via transitionless quantum driving. *Sci. Rep.* 5, 18414; doi: 10.1038/srep18414 (2015).



This work is licensed under a Creative Commons Attribution 4.0 International License. The images or other third party material in this article are included in the article's Creative Commons license, unless indicated otherwise in the credit line; if the material is not included under the Creative Commons license, users will need to obtain permission from the license holder to reproduce the material. To view a copy of this license, visit <http://creativecommons.org/licenses/by/4.0/>